

Brillouin and Raman scattering in natural and isotopically controlled diamond

R. Vogelgesang, A. K. Ramdas, and S. Rodriguez

Department of Physics, Purdue University, West Lafayette, Indiana 47907

M. Grimsditch

Argonne National Laboratory, Argonne, Illinois 60439

T. R. Anthony

GE Corporate Research and Development, Schenectady, New York 12309

(Received 22 March 1996)

The effects of zero-point motion and the anharmonicity of the lattice vibrations of diamond have been explored theoretically in the context of a valence force model explicitly incorporating the isotopic composition. The predictions are tested in a study of the elastic moduli (c_{ij}) deduced from Brillouin spectra and the zone center optical mode frequency (ω_0) from Raman spectra of isotopically controlled diamond specimens. On the basis of the anharmonicity parameter of the model associated with bond stretching, deduced from a comparison of the theory with experimentally reported dependence of the lattice parameter with the atomic fraction of ^{13}C in $^{12}\text{C}_{1-x}^{13}\text{C}_x$ diamond, it is predicted that the bulk modulus of ^{13}C diamond exceeds that for ^{12}C diamond by one part in a thousand, just below the experimental sensitivity accessible with Brillouin measurements; ω_0 exceeds the value expected from the $M^{-1/2}$ dependence, where M is the average atomic mass, by $\sim 0.3\text{ cm}^{-1}$, consistent with observation. The Grüneisen parameter for ω_0 and the third-order bulk modulus are consistent with the theoretical estimates from the present model. The elastic moduli for natural diamond determined in the present study, viz., $c_{11}=10.804(5)$, $c_{12}=1.270(10)$, and $c_{44}=5.766(5)$ in units of $10^{12}(\text{dyn}/\text{cm}^2)$ are the most accurate yet obtained. [S0163-1829(96)03330-9]

I. INTRODUCTION

The cubic modification of crystalline carbon, diamond, is characterized by a tetrahedral coordination underlying its structure dictated by the sp^3 bonding between the nearest neighbor atoms. It belongs to the space group $O_h^7 (F4_1/d\bar{3} 2/m)$ with two atoms per primitive (Bravais) cell. The strong covalent bonding and the light mass of the constituent atoms result in a large frequency for the zone center, Raman active, infrared inactive, triply degenerate F_{2g} mode.^{1,2} For the same reason, the elastic moduli of diamond are the largest known for any material and thus lead to Brillouin components with large frequency shifts. Its crystalline perfection and transparency make diamond ideally suited for inelastic light scattering studies. And indeed, soon after the discovery of the Raman effect, the first-order Raman spectrum of diamond was recorded by Ramaswamy.³ The second-order Raman spectrum of diamond was reported by Krishnan.⁴ The Brillouin components in the spectrum of the scattered light from diamond were observed by Krishnan⁴ and studied further by Chandrasekharan.⁵ Solin and Ramdas⁶ investigated the first- and second-order Raman spectra of diamond by exploiting the unique advantages of laser excitation, scanning monochromators, and photoelectric detection with the associated photon counting electronics. Grimsditch and Ramdas⁷ similarly made a comprehensive study of Brillouin scattering in diamond using a piezo-electrically scanned, multipassed, Fabry-Pérot interferometer for spectral analysis. On the basis of their investigations, they deduced the frequencies of the phonons with wave vectors corresponding to a large number of critical points of the phonon dispersion curves spanning

the entire Brillouin zone;⁶ all the elastic moduli with high precision;⁷ and an absolute Raman cross section of the zone center optical phonon from an intercomparison of the intensities of the F_{2g} Raman line and the Brillouin components recorded in the same experiment with a double monochromator.⁷

The above experiments were performed on naturally occurring diamond and hence with an isotopic composition corresponding to 98.9% ^{12}C and 1.1% ^{13}C natural abundance.⁸ The successful synthesis of diamond by the high-pressure-high-temperature (HPHT) technique (Bundy *et al.*⁹) and the low-temperature growth from the gaseous phase (Eversole¹⁰ and Derjaguin *et al.*¹¹) by chemical vapor deposition (CVD) have triggered renewed interest in the physics of diamond. In particular, the isotopic composition of the CVD diamond can now be controlled by that of the gas employed; in turn, the isotopically controlled polycrystalline diamond can be used in the HPHT technique to produce single crystals.¹² Thus an extraordinary opportunity has arisen for the study of the properties of diamond in which its isotopic composition plays a special role. Thermal conductivity,¹³ lattice parameter,¹⁴ indirect gap,¹⁵ Raman¹⁶⁻¹⁸ and Brillouin scattering,¹⁹ and multiphonon infrared absorption spectroscopy¹² are illustrative examples of a wide range of phenomena which have been investigated specifically in the context of isotopic effects. Thermal conductivity of isotopically enriched ^{12}C diamond exhibits as much as 50% enhancement at room temperature relative to that of natural diamond;¹³ this remarkable enhancement has been shown by Hass *et al.*¹⁷ and Olson *et al.*²⁰ to be due to N processes, normally ineffective, playing a special role. The

lattice constant of diamond determined by Holloway *et al.*¹⁴ exhibits a decrease linear in x , the atomic fraction of ^{13}C ; this decrease has been fully accounted for in terms of the effects of zero-point motion in conjunction with anharmonicity as was demonstrated by Buschert *et al.*²¹ in isotopically enriched germanium. Chrenko¹⁶ and Hass *et al.*¹⁷ studied the frequency of the F_{2g} zone center optical phonon (ω_0) in a series of diamond specimens which ranged in isotopic composition from $x=0.011$ to 0.99; the latter deduced x from the mass spectroscopic analysis of CO produced in the combustion of the diamonds in oxygen. The decrease in ω_0 is found to follow a predominantly $(M_x)^{-1/2}$ dependence expected from the virtual crystal approximation (VCA), the force constants being essentially independent of the isotopic composition [here $M_x = xM_{13} + (1-x)M_{12}$]. The departure from the $(M_x)^{-1/2}$ dependence has been interpreted by Hass *et al.*¹⁷ in terms of a coherent potential approximation (CPA) combined with disorder-induced mixing with phonon modes of lower frequencies.

We recently studied¹⁹ the effect of isotopic composition on the elastic moduli of a single crystal. More specifically, we compared c_{11} and $(c_{11} + 2c_{12} + 4c_{44})/3$ deduced from the Brillouin shifts produced by longitudinal acoustic waves in the back scattering geometry for several natural and a ^{13}C diamond. Based on the concentration of $^{13}\text{CH}_4$ used in its growth, the ^{13}C concentration in the latter was assumed to be $x=0.99$. The elastic moduli for the “ ^{13}C ” diamond was $\sim 0.5\%$ higher than those for natural diamond. A simple Einstein model, incorporating zero-point motion and anharmonicity, yielded expressions for the x dependence of the elastic moduli c_{ij} , the lattice parameter a , and ω_0 . The anharmonicity parameter deduced from the theoretical expression for $a(x)$, in conjunction with its experimental value yielded a satisfactory agreement with the values of ω_0 and c_{ij} 's for the $x=0.99$ ^{13}C diamond when compared to those of natural diamond. We note here that ω_0 for the “ ^{13}C ” sample was 1284.8 cm^{-1} , not 1282.1 cm^{-1} as obtained by Hass *et al.*¹⁷ for a diamond with $x=0.99$.

Since this earlier study, with a variety of isotopically controlled diamond single crystals with x ranging from 0.001 to 0.99 grown by one of us (T.R.A.), we have performed both Raman and Brillouin scattering experiments. On the basis of our new results we have to assign for the earlier “ ^{13}C ” sample a lower value of x , viz., 0.945. We have also reformulated the theory for the x dependence of ω_0 , a , and c_{ij} in terms of a lattice dynamical description for the zone center optical F_{2g} phonon and the bulk modulus, incorporating anharmonicity as well as zero-point motion. In this paper we present the theory thus reformulated, the new experimental data, and a comparison of the experimental data with the theory.

II. THEORY

From a simple thermodynamic argument, the difference in the molar volumes V and $V + \Delta V$ of two chemically identical, nonconducting crystals consisting of atoms of isotopic masses M and $M + \Delta M$, respectively, can be shown to be

$$\frac{\Delta V}{V} = -\frac{\Delta M}{2MBV} \sum_i \gamma_i \left(E_i - T \frac{\partial E_i}{\partial T} \right), \quad (1)$$

where E_i and γ_i are, respectively, the average energy at temperature T and the Grüneisen parameter of the i th phonon mode while B is the bulk modulus of the crystal.²¹ The zero-point motion and the anharmonicity enter Eq. (1) indirectly through the Grüneisen parameters. This approach does not allow one to relate the isotopic dependence of the lattice constant to those in other quantities such as ω_0 and c_{ij} .

It is, therefore, desirable to formulate a theory based on lattice dynamics which will simultaneously give expressions for isotope effects on the lattice constant, the elastic moduli, the frequency of the zone center optical phonon and the third-order bulk modulus. Lattice-dynamical theories for crystals with the diamond structure have been given by Musgrave and Pople,²² by Keating,²³ and by Martin²⁴ based on models in which the strain energy of a crystal is expressed in terms of the changes in the bond lengths and the bond angles. In this approach, called the valence-force-field method, the potential is manifestly invariant under both translations and rotations.²⁵ Anharmonic forces have been used by Keating²⁶ in a model involving two harmonic and three anharmonic force constants. In this paper we consider a simple model containing four parameters, two harmonic and two anharmonic. The harmonic part is identical to that employed by Musgrave.²⁷ Of the two anharmonic force constants, only one is of significance in our discussion, namely, the anharmonicity of the bond stretching energy.

Consider the diamond structure with lattice vectors $\mathbf{n} = (a/2)(n_1, n_2, n_3)$, where a is the conventional lattice parameter and n_1, n_2 , and n_3 are integers whose sum is even. Associated with each lattice point \mathbf{n} there is a basis of two identical atoms at $(0,0,0)$ and $(a/4, a/4, a/4)$. The nearest neighbor distance is $R = (a\sqrt{3}/4)$ and each atom has four nearest neighbors as shown in Fig. 1 where F is the atom at $(a/4, a/4, a/4)$ with nearest neighbors at $A(0,0,0)$, $B(0, a/2, a/2)$, $C(a/2, 0, a/2)$, and $D(a/2, a/2, 0)$. An arbitrary distortion of the structure can be described in terms of the vector distances between the atoms. Let \mathbf{r}_{in} be the vectors \mathbf{AF} , \mathbf{BF} , \mathbf{CF} , and \mathbf{DF} in a particular primitive cell, \mathbf{n} ; i denotes A, B, C , or D . In equilibrium, $\mathbf{r}_A^{(0)} = \mathbf{AF} = (a/4, a/4, a/4)$, $\mathbf{r}_B^{(0)} = \mathbf{BF} = (a/4, -a/4, -a/4)$, $\mathbf{r}_C^{(0)} = \mathbf{CF} = (-a/4, a/4, -a/4)$, and $\mathbf{r}_D^{(0)} = \mathbf{DF} = (-a/4, -a/4, a/4)$.

Let Δr_{in} be the change in the distance between F_n and X_{in} ($X_{in} = A_n, B_n, C_n$, or D_n) and $\Delta \theta_{ijn}$ be the change in the angle between the bonds $\mathbf{X}_{in}\mathbf{F}_n$ and $\mathbf{X}_{jn}\mathbf{F}_n$. The energy required to stretch (or contract) a bond by Δr_i is

$$\frac{1}{2} k_1 (\Delta r_i)^2 - \frac{1}{6} g_1 (\Delta r_i)^3 + \dots, \quad (2)$$

while that required to alter the angle between the bonds $\mathbf{X}_i\mathbf{F}$ and $\mathbf{X}_j\mathbf{F}$ is

$$\frac{1}{2} k_2 (R\Delta \theta_{ij})^2 - \frac{1}{6} g_2 (R\Delta \theta_{ij})^3 + \dots. \quad (3)$$

Here k_1 and k_2 are the force constants for the harmonic part of the potential, whereas g_1 and g_2 define the lowest order anharmonic contributions.

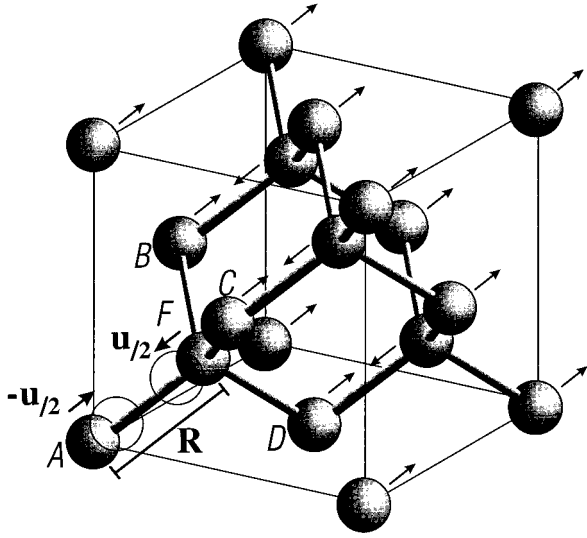


FIG. 1. The tetrahedral bonding of a carbon atom in diamond with its four nearest neighbors. \mathbf{R} is the bond length whereas \mathbf{u} , selected to be along [111], is the relative displacement of the two fcc sublattices with respect to each other in the triply degenerate F_{2g} zone center optical mode.

Neglecting interactions other than those between nearest neighbor atoms, the deformation energy is

$$\Delta U = \sum_{\mathbf{n}} \Delta U_{\mathbf{n}} = \sum_{\mathbf{n}} \left(\frac{1}{2} k_1 \sum_i (\Delta r_{in})^2 + \frac{1}{2} k_2 \sum_{i < j} (R \Delta \theta_{ijn})^2 - \frac{1}{6} g_1 \sum_i (\Delta r_{in})^3 - \frac{1}{6} g_2 \sum_{i < j} (R \Delta \theta_{ijn})^3 + \dots \right). \quad (4)$$

(a) Bulk modulus. The energy associated with the deformation in which all nearest neighbor distances change from R to $R+u$ ($u \ll R$) without change in symmetry, i.e., $\Delta r_{in} = u$ and $\Delta \theta_{ijn} = 0$ is

$$\Delta U = N \left(2k_1 u^2 - \frac{2}{3} g_1 u^3 + \dots \right), \quad (5)$$

where N is the number of primitive cells in the crystal. The change in volume is $\Delta V = (3Vu/R)$ so that

$$\Delta U = \frac{k_1 (\Delta V)^2}{6aV} - \frac{g_1 (\Delta V)^3}{72\sqrt{3}V^2} + \dots \quad (6)$$

Recalling the change in free energy F with volume

$$\Delta F = \frac{1}{2} (\Delta V)^2 \left(\frac{\partial^2 F}{\partial V^2} \right)_0 + \dots \approx \frac{(\Delta V)^2 B}{2V}, \quad (7)$$

where B is the bulk modulus. A comparison of Eqs. (6), and (7) at zero temperature yields

$$B = \frac{k_1}{3a}. \quad (8)$$

(b) Zone center optical mode. Consider a motion in which the two face-centered-cubic (fcc) sublattices of the structure experience a relative displacement u with respect to each

other, as in the F_{2g} zone center optical mode and let u be along [111], i.e., along \mathbf{AF} . The distance AF changes by u but BF, CF , and DF change by $-u/3$. Furthermore, the bond angles change from their static value $\arccos(-1/3) \cong 109^\circ$. The angles between \mathbf{AF} and \mathbf{BF} , \mathbf{AF} and \mathbf{CF} , and \mathbf{AF} and \mathbf{DF} change by $-(2\sqrt{2}u/3R)$ while those between \mathbf{BF} and \mathbf{CF} , \mathbf{CF} and \mathbf{DF} , and \mathbf{BF} and \mathbf{DF} change by $(2\sqrt{2}u/3R)$. Noting that the terms in g_2 cancel exactly, the deformation energy due to this relative displacement is

$$\Delta U = N \left[\frac{2}{3} (k_1 + 4k_2) u^2 - \frac{4g_1 u^3}{27} + \dots \right]. \quad (9)$$

The kinetic energy per primitive cell associated with the relative motion of the fcc sublattices is P^2/M where P is the momentum canonically conjugate to u and M the mass of the atom ($M/2$ being the reduced mass). Thus, the Hamiltonian per primitive cell associated with this motion is

$$\mathcal{H} = \frac{P^2}{M} + \frac{2}{3} (k_1 + 4k_2) u^2 - \frac{4g_1 u^3}{27} + \dots \quad (10)$$

Neglecting the cubic term, the equation of motion for u is harmonic with angular frequency of the F_{2g} zone center optical phonon

$$\Omega_0 = \left[\frac{8(k_1 + 4k_2)}{3M} \right]^{1/2}. \quad (11)$$

In order to estimate the effect of the zero-point motion we quantize the Hamiltonian in Eq. (10) and investigate the nature of the ground state of such a system by a variational procedure. Choosing a displaced Gaussian distribution characterized by the normalized wave function

$$\Psi(u) = \left(\frac{\alpha}{\sqrt{\pi}} \right)^{1/2} \exp \left[-\frac{\alpha^2}{2} (u - \delta)^2 \right], \quad (12)$$

where α and δ are variational parameters, one obtains the expectation value of \mathcal{H} in state $\Psi(u)$, viz.,

$$E(\alpha, \delta) = \frac{\hbar^2 \alpha^2}{2M} + \frac{2}{3} (k_1 + 4k_2) \left(\delta^2 + \frac{1}{2\alpha^2} \right) - \frac{4g_1}{27} \left(\delta^3 + \frac{3\delta}{2\alpha^2} \right) + \dots \quad (13)$$

For a given δ , the minimum of $E(\alpha, \delta)$ occurs for

$$\alpha = \left(\frac{M\Omega_0}{2\hbar} \right)^{1/2} \left(1 - \frac{16g_1 \delta}{9M\Omega_0^2} \right)^{1/4} \quad (14)$$

and

$$E(\delta) = \frac{\hbar\Omega_0}{2} + \frac{1}{4} M \omega_0^2 \left(\delta - \frac{8\hbar g_1}{9M^2 \Omega_0^3} \right)^2 - \frac{16\hbar^2 g_1^2}{81M^3 \Omega_0^4} + \dots \quad (15)$$

with

$$\omega_0 = \Omega_0 \left(1 - \frac{32\hbar g_1^2}{81M^3 \Omega_0^5} \right). \quad (16)$$

We note that the minimum of the total energy corresponds to a displacement $\delta = (8\hbar g_1/9M^2\Omega_0^3)$ with respect to the classical value obtained neglecting the kinetic energy arising from the zero-point motion of the atoms. As a result, the zone center optical phonon frequency ω_0 is the renormalized value given by Eq. (16).

(c) Bulk modulus: Effect of zero-point motion. Consider now a uniform expansion of the crystal, without altering its symmetry, but including the effect of zero-point motion. By a procedure similar to that employed above for the zone center optical phonon, one can relate additional macroscopic parameters to the microscopic parameters k_1 and g_1 . For a uniform change in volume, the Hamiltonian per primitive cell is

$$\mathcal{H} = \frac{P^2}{M} + 2k_1u^2 - \frac{2}{3}g_1u^3 + \dots \quad (17)$$

Taking a variational wave function of the form defined in Eq. (12) and minimizing the expectation value of the Hamiltonian given in Eq. (17) with respect to the parameter α , one obtains

$$E(\delta) = \hbar \left(\frac{2k_1}{M} \right)^{1/2} + 2K_1(\delta - \delta_0)^2 + \dots, \quad (18)$$

where K_1 is the renormalized stiffness constant

$$K_1 = k_1 \left(1 - \frac{\hbar g_1^2}{8\sqrt{2}k_1^{5/2}M^{1/2}} \right) \quad (19)$$

and

$$\delta_0 = \frac{\hbar g_1 \sqrt{2}}{8k_1^{3/2}M^{1/2}}. \quad (20)$$

The renormalized bulk modulus, \mathcal{B} , is then given by

$$\mathcal{B} = \frac{K_1}{3a}. \quad (21)$$

The lattice parameter is obtained from $R = R_\infty + \delta_0$ where R_∞ is the nearest neighbor distance if the atomic mass were infinitely large and hence the zero-point motion negligible. We obtain

$$a = a_\infty + \frac{\hbar g_1}{\sqrt{6}k_1^{3/2}M^{1/2}}. \quad (22)$$

III. EXPERIMENTAL PROCEDURE AND APPARATUS

A. Sample growth

Two different methods were used to prepare our diamond samples. The first method was determined solely by technical considerations while the second method took into consideration the extremely high cost of the purified ^{13}C isotope.

For samples with a low ^{13}C content, a two-stage process was used to prepare the diamond gemstones with varying isotopic compositions. First, thin polycrystalline films of pure ^{12}C and ^{13}C diamond were made by a low-pressure CVD diamond deposition process.^{10–12,28} A hot-filament

CVD apparatus was constructed out of materials such as copper and quartz containing little or no carbon to avoid contamination of the isotopically pure films. The reactor was run for 48 h with pure flowing hydrogen prior to the diamond deposition run so that atomic hydrogen generated by the hot tungsten filament at 2000 °C would remove any carbon contamination in the reactor by reacting with carbon impurities to form methane which was subsequently swept out of the reactor by the flowing hydrogen. During CVD diamond growth, isotopically pure methane²⁹ was used at a 1% concentration in a methane-hydrogen gas mixture. CVD diamond formed on a 850 °C molybdenum substrate that was spaced 8 mm from a hot tungsten filament at a temperature of 2050 °C. Diamond deposition runs were typically several hundred hours long in order to produce films approximately 100 μm thick.

On completion of the CVD diamond deposition, the films were removed from the reactor and crushed into powder and used as feed stock to grow high quality diamond gemstones. The advantage of using diamond as a feedstock instead of graphite is that there is no volume change in the diamond growth cell during crystal growth of the diamond gemstone. If graphite is used as a feedstock, there is a large volume change in the diamond growth cell as graphite (molar volume = 5.3 cm^3) converts to diamond (molar volume = 3.41 cm^3). The constancy of cell volume during crystal growth allows good control of the temperature and pressure in the cell during the 3-day growth run and ensures the steady growth rate that produces high quality diamond crystals.

The actual HPHT process as described by Strong and Wentorf³⁰ is carried out at a pressure of 55 kbars and a temperature of 1450 °C. At one end of the diamond growth cell, a diamond seed with a [001] orientation is implanted in an end plug of sodium chloride such that only the (001) facet is exposed. At the other end of the growth cell, the crushed mixture of isotopic CVD diamond is placed. Between the diamond seed and the diamond feedstock is a layer of liquid metal of 95% Fe and 5% Al by weight. The Al lowers the melting point of the mixture and getters any nitrogen in the cell to ensure that the diamond gemstone is free of nitrogen. A small temperature gradient is applied across the cell such that the CVD diamond feedstock end is 30 °C hotter than the diamond seed. The solubility of diamond in the Fe-Al liquid increases with increasing temperature. As a result, the concentration of carbon is higher at the feedstock end than at the seed end of the cell. The resulting carbon concentration gradient transports dissolved carbon atoms from the dissolving CVD feedstock to the growing diamond seed. Diamond growth rates are approximately 5.5×10^{-7} cm/sec (20 $\mu\text{m}/\text{h}$). In a typical run, 50% of the diamond feedstock is successfully converted into single crystal diamond. The remaining feedstock remains as carbon dissolved in the liquid metal, undissolved CVD feedstock or spurious secondary diamonds that nucleate randomly in the cold end of the cell.

The diamond gems are typically type IIa with a color grade of *E* on the gemological color scale (gems are graded by gemologists on a color scale ranging from *D* to *Z* with *D* being the best and rarest designation). Of all the elements, only nitrogen and boron can dissolve to any extent in diamond. The absence of any significant color implies that both

nitrogen and boron concentrations are less than 1 ppm since their concentration in excess of 1 ppm produce yellow and blue colored gems, respectively. The average size of the gems was about $4 \times 4 \times 4$ mm and average weight was 0.8 carats (1 g = 5 carats). The gem crystals typically exhibit large (001) and (111) facets and sometimes small (110) and (113) facets. All of the gems contain some small microscopic inclusions of graphite and the Fe-Al metal that were entrapped during crystal growth. The dislocation density of the crystals was determined by etching them in molten KNO_3 for 20 min in air at 650°C and found to be $10^6/\text{cm}^2$.

For samples containing significant amounts of ^{13}C carbon, economic considerations forced us to grow gem diamond directly from isotopically enriched graphite feedstock because of the much higher conversion efficiency (80%) of isotopically pure $^{13}\text{CH}_4$ to graphite in a pyrolytic cracking process³¹ as compared to the low conversion efficiency (2%) of isotopically pure $^{13}\text{CH}_4$ to diamond in the low-pressure CVD process.^{10,11} For example, the costs of just the isotopically pure $^{13}\text{CH}_4$ gas for an isotopically pure ^{13}C diamond made from CVD diamond and graphite feed stock, respectively, were \$35,000 and \$700. Consequently, in this study, the gems with compositions greater than 15% ^{13}C were grown from graphite feedstock instead of CVD diamond feedstock.

B. Raman

The 5145 Å line from an Ar^+ laser (Coherent Radiation Model 10) and the 5309 Å line from a Kr^+ laser (Spectra Physics Model 171) were used to excite Raman scattering of the samples held at room temperature. The inelastically scattered light was spectrally analyzed with a computer controlled Spex 14018 double (triple) monochromator and detected with an RCA photomultiplier tube (type C31034A) using photon counting and associated data acquisition system. For optimal mechanical reproducibility the spectrometer drive was advanced only towards lower wave numbers, scanning the laser line followed by the first-order F_{2g} Raman line. Each spectrum thus acquired was fitted with a Gaussian and Lorentzian for the laser and the Raman peak, respectively. The peak position of the Raman line could be determined reproducibly within $\pm 0.05 \text{ cm}^{-1}$.

C. Brillouin

A single moded Ar^+ laser (Coherent Radiation, Innova 90) provided the monochromatic radiation ($\lambda_L = 5145 \text{ Å}$) for exciting the Brillouin components. The scattered light was spectrally analyzed with a high contrast, piezoelectrically scanned, multipassed Fabry-Pérot interferometer.³² The high precision in the measurements of the Brillouin shifts was achieved using the interferometer without its tandem feature. The free spectral range (FSR) was set at a value for which the Brillouin components are *separated* from the parent laser line by as many as 8 full orders and a fraction of the FSR. The frequency shift is then given by $(8+f)$ FSR where f is the fraction of a free spectral range and can typically be measured with an accuracy better than ± 0.0015 . The FSR is determined with an accuracy ($\Delta\text{FSR}/\text{FSR}$) of 3×10^{-5}

using the known wavelengths from a spectral lamp.³³ The frequency shifts are thus determined with an accuracy of 0.001 cm^{-1} .

Extracting the sound velocity (v_s) from the measured frequency shift requires knowledge of the refractive index n and the scattering angle θ . Uncertainty in the latter leads to an error in the wave vector $|\mathbf{q}|$. In our case the uncertainty arising from the finite collection aperture leads to $(\Delta q/q) = 7 \times 10^{-5}$. This error is systematic and affects all our measurements in the same fashion and hence has no effect on the intersample comparison presented here. Errors due to uncertainty in the refractive index (numerical values are given in Sec. IV) fall into the same category. There could be a systematic error due to the value chosen for natural diamonds; this error again does not affect our intercomparison. We have however made a correction to the refractive index to account for density changes between samples with different isotopic constitution. Uncertainties arising from corrections to the refractive index are negligible. Thus $(\Delta v_s/v_s)$ is ≈ 0.00025 .

The final step in extracting the elastic moduli involves the density of the samples. Here again any error in the density chosen for natural diamond will contribute only a systematic error. However, the uncertainties in the ^{13}C concentration (x) will introduce uncertainty in the density. The overall accuracy in the elastic moduli (X) is $(\Delta X/X) = 2(\Delta v_s/v_s) + (\Delta x/12) = 0.0005 + (\Delta x/12)$.

The Brillouin experiments were performed in the back-scattering geometry for phonon propagation vectors \mathbf{q} along [001], [111], and [110]. The incident beam was normal to the sample surface; by adjusting the retroreflected beam to be collinear with the incident beam over a distance of more than 30 cm, this was accurate to within 1° . Since the facets produced during growth for natural and synthetic diamonds are *exactly* normal to the desired direction, single measurements are sufficient to determine the Brillouin shift for each particular wavevector. (This fact was also verified experimentally on a number of samples.) For diamond surfaces which had been prepared by polishing, and hence possibly misoriented by a few degrees, the Brillouin shift was measured for the various propagation directions close to the surface normal. (Note that this does not change the scattering angle θ .) Since the frequency shift is an *extremum* along the three symmetry directions considered, the procedure leads to plots similar to those shown in Fig. 2 where the Brillouin shifts as function of angle for \mathbf{q} in the vicinity of [111] and [001] are depicted for samples with polished surfaces, clearly showing the occurrence of extrema along the desired crystallographic directions for \mathbf{q} ; here the departure from the desired \mathbf{q} is $\sim 5^\circ$. Figure 3(a) shows the Brillouin components recorded in first order, the tandem feature being operational in the Fabry-Pérot interferometer. Those recorded without the tandem feature and in high interference order are displayed in Figs. 3(b) and 3(c).

IV. EXPERIMENTAL RESULTS AND ANALYSIS

A. Raman spectra: Isotopic composition

The first-order Raman spectrum, i.e., the Raman line associated with the zone center F_{2g} mode (ω_0), is of fundamental importance in the context of the theme of the present

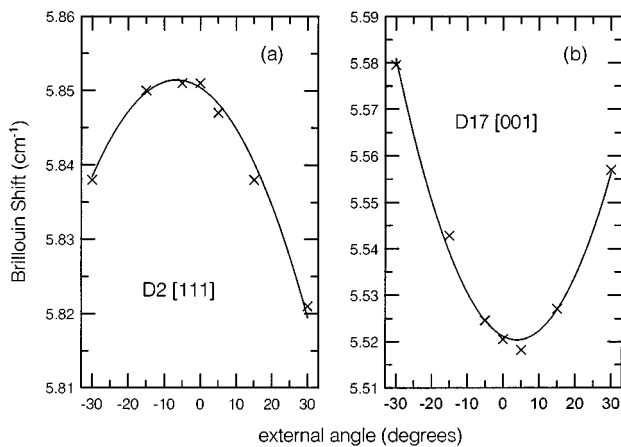


FIG. 2. Brillouin shift as a function of the external angle of the scattering direction with respect to the normal of a polished surface. The solid line is a polynomial fit from which the extremum of the Brillouin shift is extracted.

investigation. On the one hand, one can establish a calibration for the isotopic composition on the basis of the position of the Raman line, as was indeed accomplished by Hass *et al.*¹⁷ (This required the “destructive” mass spectroscopic analysis of the CO produced by the combustion of the diamonds in oxygen.³⁴) On the other hand, the x dependence of ω_0 includes contributions from the combined effects of zero-point motion and the anharmonicity as deduced in Sec. II. In view of these considerations we made a careful study of the first-order Raman spectra of all the diamond specimens available to us.

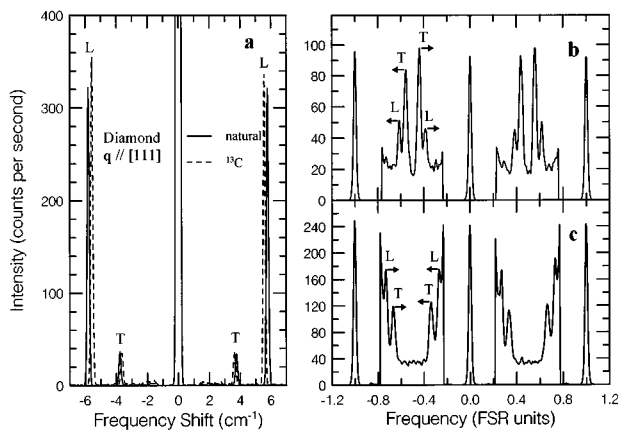


FIG. 3. Brillouin spectra of natural and isotopically enriched diamonds. (a) The spectra were recorded in the backscattering geometry for 5145 Å radiation incident along [111] and the backscattered light analyzed with a (5+4) tandem Fabry-Pérot interferometer. The phonon wave vector is along [111]. Here L and T denote longitudinal and transverse, respectively. (b) Brillouin spectrum for ^{13}C diamond in the same geometry as for (a) but analyzed with a five-pass interferometer with a FRS of $0.670\,67\text{ cm}^{-1}$, and with an analyzer in the scattered beam to reduce the intensity of the longitudinal peaks. The longitudinal L and transverse T peaks are ≈ 8.4 and ≈ 5.4 orders from their parent laser line as indicated by the arrows. (c) Same as (b) but for ^{12}C diamond. The L and T peaks are now ≈ 8.7 and ≈ 5.7 orders from their parent line, respectively.

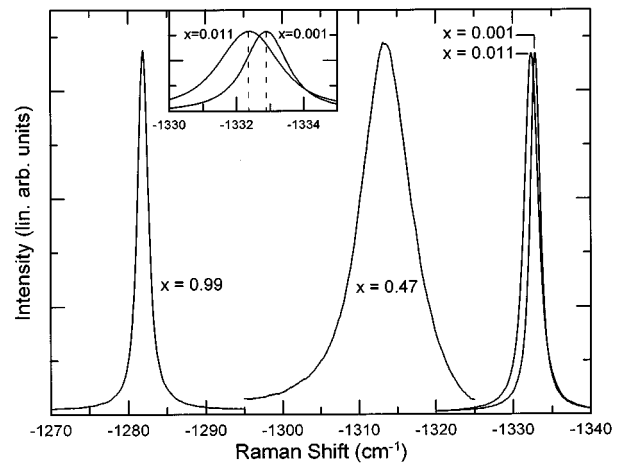


FIG. 4. The first-order Raman spectra of diamond specimens for $x = 0.001$, $x = 0.011$, $x = 0.47$, and $x = 0.99$.

In Fig. 4 we display the F_{2g} Raman line for four specimens with isotopic compositions corresponding to $x = 0.001, 0.011, 0.47$, and 0.99 , where we quote the “nominal” values for x . The peak positions of the Raman line for seven natural diamonds (five type IIa and two type IIb) yielded a value of $1332.40 \pm 0.05\text{ cm}^{-1}$. The positions for the synthetic diamonds are listed in Table I. It is of interest to note that the natural abundances of the stable isotopes of carbon, viz. ^{12}C and ^{13}C , correspond to $x = 0.0110$ as quoted by DeLaeter *et al.*⁸ with the “warning” that a more accurate assessment of the natural abundance may be necessary for high precision experiments. In this context the following comment by Orlov³⁵ on natural diamonds is significant: “On the basis of these investigations, we can state the following conclusion. The isotope composition of carbon in diamond crystals (irrespective of their variety) and in coarse-grained bort is approximately the same. The $\text{C}^{12}/\text{C}^{13}$ ratios for these varieties vary within a narrow range: 89.24 to 89.78.” We have thus ascribed to all the natural specimens used in the present study a value of $x_{\text{nat}} = 0.011\,05(3)$ and assign the value $\omega_0 = 1332.40(5)\text{ cm}^{-1}$ to the zone center optical phonon frequency of natural diamond.

On the basis of the data of Hass *et al.*¹⁷ and that for natural diamond, the following polynomial fit can be established for $\omega_0(x)$:

TABLE I. The ^{13}C molar fraction (x) in the $^{12}\text{C}_{1-x}^{13}\text{C}_x$ diamond specimens deduced from the measured Raman shift of the zone center optical phonon, according to Eq. (24).

Sample	x (nominal)	Observed Raman shift (cm^{-1})	x (calculated)
D27	0.001	1332.72	0.003(3)
D29	0.001	1332.88	-0.002(3)
D25	0.001	1332.87	-0.002(3)
D35 ^a	0.011	1332.20	0.018(3)
D28	0.47	1313.44	0.456(5)
D24	0.99	1284.80	0.945(2)
D30	0.99	1281.63	0.992(2)
D31	0.99	1281.61	0.992(2)

^aSynthetic type-I diamond of natural composition.

TABLE II. Brillouin frequency shifts $\Delta\omega$, squares of sound velocities $v^2=X/\rho$, and elastic moduli X as measured for various ^{13}C concentrations and phonon wave vectors \mathbf{q} .

\mathbf{q} ; polarization	Sample	x	$\Delta\omega$ (cm^{-1})	X/ρ 10^{12} (cm/sec) 2	X 10^{12} dyn/cm^2
[111]; LA $X=\frac{1}{3}(c_{11}+2c_{12}+4c_{44})$	D29	0.0	5.855(1)	3.458(1)	12.143(5)
	D25	0.0	5.854(1)	3.457(1)	12.139(5)
	D2	0.01105	5.851(1)	3.452(1)	12.136(5)
	D28	0.456	5.748(1)	3.332(1)	12.150(10)
	D24 ^a	0.945	5.636(1)	3.203(1)	12.142(10)
	D30	0.992	5.623(1)	3.188(1)	12.131(7)
[111]; TA $X=\frac{1}{3}(c_{11}-c_{12}+c_{44})$	D29	0.0	3.799(1)	1.455(1)	5.111(3)
	D2	0.01105	3.793(1)	1.451(1)	5.100(3)
	D30	0.992	3.648(1)	1.342(1)	5.107(5)
[001]; LA $X=c_{11}$	D29	0.0	5.522(1)	3.075(1)	10.799(5)
	D25	0.0	5.521(1)	3.075(1)	10.798(5)
	D17	0.01105	5.520(1)	3.073(1)	10.804(5)
	D28	0.456	5.422(1)	2.964(1)	10.810(10)
	D24	0.945	5.317(1)	2.850(1)	10.806(10)
	D30	0.992	5.304(1)	2.837(1)	10.793(7)
[110]; LA $X=\frac{1}{2}(c_{11}+c_{12}+2c_{44})$	D29	0.0	5.773(1)	3.362(1)	11.806(5)
	D1	0.01105	5.770(1)	3.358(1)	11.804(5)
	D30	0.992	5.545(1)	3.100(1)	11.796(7)
	D31	0.992	5.545(1)	3.100(1)	11.796(7)

^aPreviously believed to be $x=0.99$ diamond.

$$\omega_0(x) = 1332.82 - 34.77x - 16.98x^2. \quad (23)$$

B. Brillouin scattering

Viewing light scattering from long wavelength acoustic phonons to be a consequence of the Bragg reflections from the optical stratifications produced by them, one can show⁷ that the Doppler shifts of the Brillouin components in a cubic crystal are

$$\Delta\omega = \pm 2\omega_L n \frac{v_s}{c} \sin\left(\frac{\theta}{2}\right). \quad (24)$$

Here ω_L is the frequency of the incident laser radiation; n , the refractive index of the scattering medium; c , the speed of light in vacuum; θ , the scattering angle; and v_s , the velocity of the sound wave responsible for the Bragg reflection. The appropriate combinations (X 's) of the elastic moduli (c_{ij}) are given by

$$X = v_s^2 \rho, \quad (25)$$

where ρ is the mass density. We express the ^{13}C concentration dependent mass density ρ by $\rho(x) = 8M_x/a(x)^3$, where $a(x)$ has been determined by Holloway *et al.*¹⁴ to be

$$a(x) = (3.56715 - 0.00053x) \text{ \AA}. \quad (26)$$

The calculated $\rho(x_{\text{nat}}) = 3.5152(1) \text{ g}/\text{cm}^3$ based on Eq. (26) compares very well with $3.5153 \text{ g}/\text{cm}^3$ quoted by Mykola-jewycz *et al.*³⁶ [The value of $\rho(x_{\text{nat}})$ used in Ref. 7, $3.512 \text{ g}/\text{cm}^3$, quoted from McSkimin and Bond,³⁷ should be taken into account while comparing the elastic moduli given in

Refs. 7, 19, 37, and 38, on the one hand, and those in the present paper on the other, i.e., values in the former should be increased by a factor of 1.00094.] From the known elasto-optic constants of natural diamond⁷ and the change in lattice parameter, a linear interpolation for the index of refraction yields $n(x) = 2.42930 + 0.00017x$. For the backscattering geometry ($\theta = 180^\circ$) employed in the present study, the experimentally determined elastic modulus X is thus given by

$$X(x) = \frac{c^2}{4\omega_L^2} \frac{\rho(x)}{n^2(x)} \Delta\omega^2(x). \quad (27)$$

The scattering intensity for the longitudinal acoustic (LA) Brillouin components in the backscattering geometry is non-zero for (i) $\mathbf{q} \parallel [001]$, (ii) $\mathbf{q} \parallel [110]$, and (iii) $\mathbf{q} \parallel [111]$; for transverse acoustic (TA) phonons with these \mathbf{q} 's it is nonzero only for (iv) $\mathbf{q} \parallel [111]$. All four cases have been investigated and the results are tabulated in Table II. The corresponding X , i.e., combinations of the elastic moduli c_{ij} , for these cases are

$$X^{(i)} = c_{11},$$

$$X^{(ii)} = \frac{c_{11} + c_{12} + 2c_{44}}{2},$$

$$X^{(iii)} = \frac{c_{11} + 2c_{12} + 4c_{44}}{3}, \quad (28)$$

$$X^{(iv)} = \frac{c_{11} - c_{12} + c_{44}}{3}.$$

V. DISCUSSION

In the theoretical approach formulated in Sec. II, a single parameter, viz., g_1 , controls all anharmonic effects. It is thus of interest to establish the validity of the model in correlating a variety of isotope related effects. In addition, it is worth exploring the relevance of the model in accounting for other phenomena in which anharmonicity plays a role.

(a) Lattice parameter and the anharmonicity constant. The concentration dependent lattice parameter incorporating zero-point motion in combination with anharmonicity, deduced from Eq. (22), is

$$a(x) = a_{12} - \frac{\hbar g_1}{(6k_1^3 M_{12})^{1/2}} \left[1 - \left(\frac{M_{12}}{M_x} \right)^{1/2} \right] \quad (29)$$

with $M_x = (1-x)M_{12} + xM_{13}$. A comparison of Eq. (29) with the data of Holloway *et al.*¹⁴ for $a(x)$ and $k_1 = 3Ba = 4.76 \times 10^5$ dyn/cm for natural diamond yields $g_1 = (4.5 \pm 0.4) \times 10^{14}$ erg/cm³. Yamanaka *et al.*³⁹ have recently reported results on a remeasurement of the influence of isotopic composition on the lattice parameter of diamond. Their data analyzed in the same manner yields $g_1 = (4.7 \pm 0.4) \times 10^{14}$ erg/cm³. The departure from the experimental linear x dependence of a expected from Eq. (22) is no more than 10^{-5} Å in the range of $x=0$ to $x=1$, i.e., well below the experimental error.

(b) Raman frequency as a function of concentration. From Eqs. (11) and (16) the concentration dependence of ω_0 , the zone center optical phonon frequency, within the virtual crystal approximation is

$$\frac{\omega_0(x)}{\omega_0(0)} = \left(\frac{M_{12}}{M_x} \right)^{1/2} \left[1 + \frac{32\hbar g_1^2}{81M_{12}^3 \omega_0(0)^5} \left\{ 1 - \left(\frac{M_{12}}{M_x} \right)^{1/2} \right\} \right], \quad (30)$$

keeping corrections to the second power of g_1 only.

As pointed out by Hass *et al.*¹⁷ and Spitzer *et al.*,¹⁸ the isotopic disorder produces a phonon lifetime proportional to $x(1-x)$ accompanied by a shift in the real part of the frequency of the form $Cx(1-x)$. The justification for this result is as follows. The deviation of the scattering potential V_{12} or V_{13} from its average $(1-x)V_{12} + xV_{13}$ is $x(V_{13} - V_{12})$ in the vicinity of a ¹²C atom and $(1-x) \times (V_{12} - V_{13})$ around ¹³C. The average lifetime is then proportional to $[(1-x)x^2 + x(1-x)^2](V_{13} - V_{12})^2 = x(1-x) \times (V_{13} - V_{12})^2$. The shift of ω_0 follows from the Kramers-Kronig relations and from its imaginary part (lifetime).

We add, therefore, $Cx(1-x)$ to Eq. (30), where C is an adjustable parameter. The Taylor expansion of

$$\omega_0(x) = \omega_0(0) \left(\frac{M_{12}}{M_x} \right)^{1/2} \left[1 + \frac{32\hbar g_1^2}{81M_{12}^3 \omega_0(0)^5} \left\{ 1 - \left(\frac{M_{12}}{M_x} \right)^{1/2} \right\} \right] + Cx(1-x) \quad (31)$$

is consistent with Eq. (23) with $C = 20.4$ cm⁻¹. The neglect of the second term in the square brackets of Eq. (31), i.e., the correction associated with zero-point motion, yields a (mar-

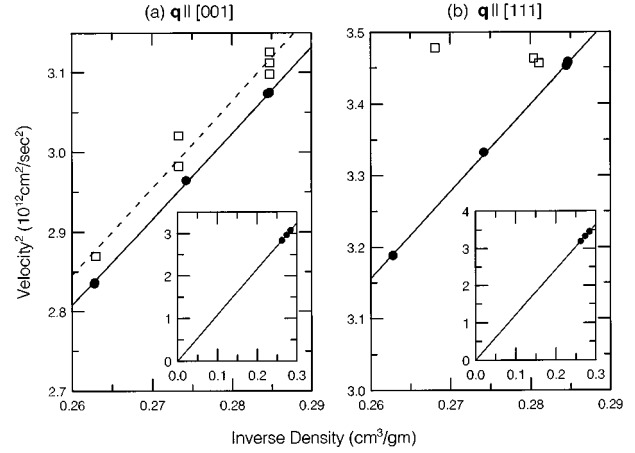


FIG. 5. v_s^2 vs $\rho^{-1}(x)$ for longitudinal acoustic phonons traveling along [001] and [111] in diamond specimens of varying isotopic composition. Our data points are indicated by solid circles; the solid line represents a linear least squares fit passing through the origin [$\rho^{-1}(x)=0$]. The data points from Tables II and IV of Hurley *et al.* (Ref. 44) are represented by open squares; the dashed line passing through their data points is again a linear least squares fit passing through the origin.

ginally) less satisfactory representation of the data. The experimental reports on $\omega_0(x)$ in the literature (Chrenko¹⁶ and Spitzer *et al.*¹⁸) are in general consistent with Eq. (23). The disorder-induced term in Eq. (31), vanishes at $x=0$ and $x=1$; the departure of $\omega_0(^{13}\text{C})/\omega_0(^{12}\text{C})$ from $(M_{12}/M_{13})^{1/2}$, i.e., from VCA, is a measure of the contribution due to the zero-point motion. While VCA yields 1280.6 cm⁻¹ for $\omega_0(^{13}\text{C})$, Eq. (31) predicts 1280.9 cm⁻¹ in reasonable agreement with 1281.07 cm⁻¹ from the polynomial fit to the Raman data, Eq. (23).

(c) Elastic moduli. In Table II we display the results of the Brillouin measurements for the four directions of phonon wave vectors investigated. The squares of the velocity of sound clearly show a decrease with increasing average mass. The corresponding elastic moduli X are calculated according to Eq. (27). An inspection of the last column of Table II reveals, within the experimental accuracy, no systematic dependence of X on the isotopic composition. Thus a plot of v_s^2 as a function of $\rho^{-1}(x)$ should yield a straight line passing through the origin; indeed, such a representation of the data can be used to detect any x dependence of c_{ij} . We display such plots in Fig. 5 for $\mathbf{q} \parallel [001]$ and $[111]$, yielding $\langle c_{11} \rangle = 10.798$ and $\langle c_{11} + 2c_{12} + 4c_{44} \rangle / 3 = 12.140$, in units of 10^{12} dyn/cm², respectively.

From the data obtained it is possible to determine c_{11} , c_{12} , and c_{44} separately for $x=0.0$, $x=0.01105$ and $x=0.992$. The results are displayed in Table III. From these elastic moduli one can deduce the bulk modulus, the values being given in the last column of Table III. The theoretical prediction for $\mathcal{B}(x)$ is

$$\frac{\mathcal{B}(x)}{\mathcal{B}(0)} = \frac{a(0)}{a(x)} \left[1 + \frac{\hbar g_1^2}{8(2k_1^5 M_{12})^{1/2}} \left\{ 1 - \left(\frac{M_{12}}{M_x} \right)^{1/2} \right\} \right] \approx 1 + 0.0012x \quad (32)$$

TABLE III. Elastic moduli c_{ij} and bulk modulus \mathcal{B} of diamond (in units of 10^{12} dyn/cm²).

x	Sample	c_{11}	c_{12}	c_{44}	\mathcal{B}
0.0	D29	10.799(5)	1.248(10)	5.783(5)	4.432(8)
0.01105	D1, D2, and D17	10.804(5)	1.270(10)	5.766(5)	4.448(8)
0.992	D30	10.792(7)	1.248(14)	5.776(7)	4.429(12)

with the values of k_1 and g_1 used above. Thus the accuracy of the present Brillouin measurements does not allow the detection of $\sim 0.1\%$ increase in \mathcal{B} expected from theory for $\mathcal{B}^{(12\text{C})}/\mathcal{B}^{(13\text{C})}$.

(d) Anharmonic effects. The Grüneisen parameter for the zone center optical phonon of diamond, measured by Parsons⁴⁰ and by Grimsditch *et al.*,⁴¹ are 1.19 ± 0.09 and 1.06 ± 0.08 , respectively. Within the theory presented in this paper the Grüneisen parameter can be deduced as

$$\gamma = -\frac{\partial(\ln\omega_0)}{\partial(\ln V)} = -\frac{\partial\ln\omega_0}{\partial g_1} \left[\frac{\partial(\ln V)}{\partial g_1} \right]^{-1} = \frac{64\sqrt{2}g_1 a}{27M\omega_0^5} \left(\frac{Ba}{M} \right)^{3/2}. \quad (33)$$

Thus for diamond $\gamma = 4.2 \times 10^{-15} g_1 = 1.9$. While this value is qualitatively consistent with that experimentally obtained, the significance of the difference needs to be understood.

The thermal average of the displacement u in Eq. (17) yields the coefficient of volume thermal expansion β as

$$\beta = \frac{1}{V} \left(\frac{\partial V}{\partial T} \right)_P = \frac{g_1 k_B \sqrt{3}}{2k_1^2 a} \frac{(y/2)^2}{\sinh^2(y/2)}, \quad (34)$$

where

$$y = \frac{\hbar}{k_B T} \left(\frac{8k_1}{M} \right)^{1/2}. \quad (35)$$

This yields $\beta = 2.7 \times 10^{-6} \text{ K}^{-1}$ at 1000 K. The linear thermal expansion coefficient α has been measured by Slack *et al.*⁴² to be $4.4 \times 10^{-6} \text{ K}^{-1}$ at 1000 K, which would imply a volume expansion coefficient of $\beta = 13.2 \times 10^{-6} \text{ K}^{-1}$. This value is markedly higher than that predicted and calls for investigation of other contributing factors.

The third-order bulk modulus \mathcal{B}' can be expressed in terms of the anharmonicity parameter g_1 . We obtain

$$\mathcal{B}' = \frac{d\mathcal{B}}{dP} = -\frac{V}{\mathcal{B}} \left(\frac{\partial \mathcal{B}}{\partial g_1} \right) \left(\frac{\partial V}{\partial g_1} \right)^{-1} = \frac{g_1}{12\sqrt{3}\mathcal{B}} = \frac{g_1 a}{4\sqrt{3}k_1} = 4.9. \quad (36)$$

Assuming the bulk modulus to be a linear function of the pressure, one obtains the Murnaghan equation of state

$$\frac{V_0}{V} = \left(1 + P \frac{\mathcal{B}'_0}{\mathcal{B}_0} \right)^{1/\mathcal{B}'_0}, \quad (37)$$

where \mathcal{B}'_0 is the derivative of the bulk modulus with respect to pressure, evaluated for $P=0$. With the experimentally determined value⁴³ $\mathcal{B}'_0 = 4.03$ we conclude that the molar volume of ¹²C diamond equals that of ¹³C diamond at zero pressure when $P=0.2$ GPa. The bulk modulus of ¹³C diamond at zero pressure must equal that of ¹²C diamond at 0.2 GPa. We thus conclude that

$$\frac{\mathcal{B}^{(13\text{C})} - \mathcal{B}^{(12\text{C})}}{\mathcal{B}^{(12\text{C})}} = 1.8 \times 10^{-3} \quad (38)$$

in reasonable agreement with our previous estimate using Eq. (32).

VI. COMPARISONS WITH PREVIOUS WORK

(a) Elastic moduli of natural diamond. The elastic moduli in Tables II and III must be compared with values in Refs. 7, 19, and 38. After accounting for the more accurate density used in this paper (which introduces the factor of 1.000 94) our present values are in excellent agreement with those in Refs. 19 and 38. Also, except for the value of c_{11} , they agree with those in Ref. 7. Based on the reproducibility of our current results on various samples we conclude that the (density-scaled) value of c_{11} in Ref. 7 (10.774 ± 0.002) should be superseded by 10.802 ± 0.005 obtained from Ref. 19 and this work. We also note that the accuracy of c_{12} and c_{44} in the present study is improved over that achieved in Ref. 7 because the transverse modes were observed in a backscattering geometry. The values for c_{ij} 's in Table II for natural diamonds are the most accurate to date.

(b) Elastic moduli of ¹³C diamond. The results in the present paper must be compared with those of Refs. 19 and 46. In Ref. 19 the c_{ij} 's of ¹³C diamond relied on what turns out to be an overestimate of x . Using the correct x , the values in Ref. 19 incorporated in Table II show no effect due to isotopic composition. In Ref. 19 it was also found that the isotopic hardening could be understood on the basis of a simple model. The theoretical estimate used in Ref. 19 was based on a simplified model in which the atoms vibrate about their equilibrium positions independently of one another, i.e., following the Einstein model including anharmonicity. The calculation predicted correctly a linear decrease with x of the lattice parameter, an increase in ω_0 over and above the $M^{-1/2}$ dependence and an increase in the bulk modulus. In the context of the present analysis of the isotope effects in diamond, the previous approach overestimated the *residual* effects in ω_0 (¹³C) and c_{ij} 's by a factor of ~ 4 .

Recently Hurley *et al.*⁴⁴ reported ultrasonic velocity determination in isotopically controlled diamonds with x ranging from ~ 0 to 0.99. They have measured the velocity of longitudinal and transverse sound waves for \mathbf{q} along [001] as well as [111]. In Fig. 5 we also display the data of Hurley *et al.*⁴⁴ Their data would yield $\langle c_{11} \rangle = 10.944 \times 10^{12}$ dyn/cm², when analyzed in the same manner as in this paper. For $\mathbf{q} \parallel [111]$ such an analysis does not appear reasonable in view of the essential constancy of v_s in Table III of their paper; the large c_{12} deduced by them for $x=0.99$ in comparison to that for $x \sim 0$, viz. 2.379×10^{12} dyn/cm² vs 1.252×10^{12} dyn/cm², respectively, arises in the main from their $v_s^{(111)}$ for

$x=0.99$. The nearly factor of 2 increase in the value c_{12} reported by them, in contrast to the constancy with x observed by us, is very puzzling.⁴⁵ We also note here that, contrary to the remark in Hurley *et al.*,⁴⁴ backscattering along [111] allows *both* longitudinal and transverse acoustic phonon modes to generate Brillouin components with relative intensities of $(p_{11}-p_{12}-2p_{44})^2/(p_{11}+2p_{12}-2p_{44})^2$, where p_{11} , p_{12} and p_{44} are the elasto-optic constants. This ratio can be deduced from Table I of Ref. 7 for $\mathbf{q} \parallel [111]$; note the doubly degenerate transverse modes appear in parallel as well as in cross polarization, whereas the longitudinal occurs only in the parallel polarization.

VII. CONCLUDING REMARKS

We have developed a model of anharmonic effects in tetrahedrally coordinated materials and used it to analyze the effects of isotopic constitution on material parameters. The model correctly accounts for the Grüneisen parameter of the zone center phonon and the third-order bulk modulus. When applied to the effects of zero-point motion, it predicts changes in the lattice constant, frequency of the zone center optical phonon, and elastic moduli.

Here we note that Ω_0 calculated from Eq. (11), neglecting $4k_2$ in comparison to k_1 , is $(8Ba/M)^{1/2}$, yielding 1336.8 cm^{-1} for natural diamond, 507 cm^{-1} for Si and 282 cm^{-1} for Ge. These are to be compared to the experimentally observed Raman shifts of 1332.4 , 519 , and 304.5 cm^{-1} , for

diamond, Si (Ref. 46), and Ge (Ref. 47), respectively. It thus appears that the force constants for bond stretching dominate those for bond bending.

The isotope effect on the lattice constant has been observed by Holloway *et al.* and is used to determine the single anharmonicity parameter of the model (g_1). The magnitude of the resulting changes in Raman frequency and elastic moduli lie just beyond the range of the Raman and Brillouin experiments reported here.

The value of a_∞ in Eq. (22), the lattice parameter in the absence of zero-point motion, obtained from a fit of the variation of the lattice parameter with x , is 3.5542 \AA . If ^{14}C diamond could be synthesized, its lattice constant would be 3.5662 \AA , using M_{14} for M ; the bulk modulus would not significantly differ from that of diamond composed of stable isotopes of carbon. The deviation of ω_0 from the $M^{-1/2}$ dependence is expected to be $\sim 1 \text{ cm}^{-1}$ with respect to that of ^{12}C diamond.

ACKNOWLEDGMENTS

The authors thank M. Cardona for stimulating discussions. The work reported in this paper received support from the National Science Foundation (Grant No. DMR 93-03186) at Purdue University and from the U.S. Department of Energy, BES Material Sciences (Grant No. W-31-109-ENG-38) at the Argonne National Laboratory.

-
- ¹N. S. Nagendra Nath, Proc. Ind. Acad. Sci. **1**, 333 (1934).
²T. Venkatarayudu, Proc. Ind. Acad. Sci. A **8**, 349 (1938).
³C. Ramaswamy, Ind. J. Phys. **5**, 97 (1930).
⁴R. S. Krishnan, Proc. Ind. Acad. Sci. A **26**, 399 (1947).
⁵V. Chandrasekharan, Proc. Ind. Acad. Sci. A **32**, 379 (1950).
⁶S. A. Solin and A. K. Ramdas, Phys. Rev. B **1**, 1687 (1970).
⁷M. H. Grimsditch and A. K. Ramdas, Phys. Rev. B **11**, 3139 (1975).
⁸J. R. De Laeter, K. G. Heumann, and K. J. R. Rosman, J. Phys. Chem. Ref. Data **20**, 1327 (1991).
⁹F. P. Bundy, H. T. Hall, H. M. Strong, and R. H. Wentorf, Nature **176**, 51 (1955).
¹⁰W. G. Eversole, U.S. Patent Nos. 3030187 and 3030188, 1962.
¹¹B. V. Derjaguin, D. V. Fedoseev, V. M. Lukyanovich, B. V. Spitzin, V. A. Ryabov, and A. V. Lavrentyev, J. Cryst. Growth **2**, 380 (1968).
¹²T. R. Anthony and W. F. Banholzer, Diam. Relat. Mater. **1**, 717 (1992).
¹³T. R. Anthony, W. F. Banholzer, J. F. Fleischer, L. Wei, P. K. Kuo, R. L. Thomas, and R. W. Pryor, Phys. Rev. B **42**, 1104 (1990).
¹⁴H. Holloway, K. C. Hass, M. A. Tamor, T. R. Anthony, and W. F. Banholzer, Phys. Rev. B **44**, 7123 (1991).
¹⁵A. T. Collins, S. C. Lawson, G. Davies, and H. Kanda, Phys. Rev. Lett. **65**, 891 (1990).
¹⁶R. M. Chrenko, J. Appl. Phys. **63**, 5873 (1988).
¹⁷K. C. Hass, M. A. Tamor, T. R. Anthony, and W. F. Banholzer, Phys. Rev. B **45**, 7171 (1992).
¹⁸J. Spitzer, P. Etchegoin, M. Cardona, T. R. Anthony, and W. F. Banholzer, Solid State Commun. **88**, 509 (1993).
¹⁹A. K. Ramdas, S. Rodriguez, M. Grimsditch, T. R. Anthony, and W. F. Banholzer, Phys. Rev. Lett. **71**, 189 (1993).
²⁰J. R. Olson, R. O. Pohl, J. W. Vandersande, A. Zoltan, T. R. Anthony, and W. F. Banholzer, Phys. Rev. B **47**, 14 850 (1993).
²¹R. C. Buschert, A. E. Merlini, S. Pace, S. Rodriguez, and M. H. Grimsditch, Phys. Rev. B **38**, 5219 (1988).
²²M. J. P. Musgrave and J. A. Pople, Proc. R. Soc. London, Ser. A **268**, 474 (1962).
²³P. N. Keating, Phys. Rev. **145**, 637 (1966).
²⁴R. M. Martin, Phys. Rev. B **1**, 4005 (1970).
²⁵M. Lax, in *Lattice Dynamics*, edited by R. F. Wallis (Pergamon, New York, 1965), p. 583.
²⁶P. N. Keating, Phys. Rev. **149**, 674 (1966).
²⁷M. J. P. Musgrave, *Crystal Acoustics* (Holden-Day, San Francisco, 1970), pp. 248–257.
²⁸J. C. Angus and C. C. Hayman, Science **241**, 913 (1988).
²⁹Obtained from Cambridge Isotope Laboratories Inc., Woburn, MA 01801.
³⁰H. M. Strong and R. H. Wentorf, Am. J. Phys. **59**, 1005 (1991).
³¹T. R. Anthony, J. C. Bradley, P. J. Horoyksi, and M. L. W. Thewalt (unpublished).
³²J. R. Sandercock, in *Proceedings of the VIIth International Conference on Raman Spectroscopy, Ottawa, Canada 1980*, edited by W. F. Murphy (North-Holland, Amsterdam, 1980), p. 364.
³³In our FSR calibration we used the 5769.5982 \AA and 5790.6630 \AA lines from a low-pressure Hg calibration lamp and the 5764.4188 \AA , 5852.4878 \AA , and 5881.8950 \AA lines from a Ne lamp. In both cases these lines were isolated from the rest of the

- emission spectrum by an interference filter centered at 5800 Å with 100 Å bandpass.
- ³⁴W. F. Banholzer and T. R. Anthony, *Thin Solid Films* **212**, 1 (1992).
- ³⁵Y. L. Orlov, *The Mineralogy of the Diamond* (John Wiley, New York, 1973), p. 30.
- ³⁶R. Mykolajewycz, J. Kalnajs, and A. Smakula, *J. Appl. Phys.* **35**, 1773 (1964).
- ³⁷H. J. McSkimin and W. L. Bond, *Phys. Rev.* **105**, 116 (1957).
- ³⁸H. J. McSkimin, P. Andreatch, Jr., and P. Glynn, *J. Appl. Phys.* **43**, 985 (1972).
- ³⁹T. Yamanaka, S. Morimoto, and H. Kanda, *Phys. Rev. B* **49**, 9341 (1994).
- ⁴⁰B. J. Parsons, *Proc. R. Soc. London, Ser. A* **352**, 397 (1977).
- ⁴¹M. H. Grimsditch, E. Anastassakis, and M. Cardona, *Phys. Rev. B* **18**, 901 (1978).
- ⁴²G. A. Slack and S. F. Bartram, *J. Appl. Phys.* **46**, 89 (1975).
- ⁴³H. J. McSkimin and P. Andreatch, *J. Appl. Phys.* **43**, 2944 (1972).
- ⁴⁴D. C. Hurley, R. S. Gilmore, and W. F. Banholzer, *J. Appl. Phys.* **76**, 7726 (1994).
- ⁴⁵We have recently become aware of work on the lattice constants of ¹²C and ¹³C diamond as a function of hydrostatic pressure [H. Fujihisa, V. A. Sidorov, K. Takemika, H. Kanda and S. M. Stishov (private communication)]. Their data are consistent with the bulk modulus of natural diamond and do not show the 17% change reported by Hurley *et al.* (Ref. 44).
- ⁴⁶P. A. Temple and C. E. Hathaway, *Phys. Rev. B* **7**, 3685 (1973).
- ⁴⁷H. D. Fuchs, C. H. Grien, C. Thomsen, M. Cardona, W. L. Hansen, E. E. Haller, and K. Itoh, *Phys. Rev. B* **43**, 4835 (1991).